FEBS Letters 580 (2006) 904–911

A novel yeast two-hybrid approach to identify CDPK substrates: Characterization of the interaction between AtCPK11 and AtDi19, a nuclear zinc finger protein[1]

Miguel A. Rodriguez Milla[a], Yuichi Uno[b], Ing-Feng Chang[a], Jared Townsend[a], Eileen A. Maher[c], David Quilici[a], John C. Cushman[a,*]

[a] *Department of Biochemistry and Molecular Biology, MS 200, University of Nevada, Reno, NV 89557-0014, USA*
[b] *Plant Resource Science, Department of Agriculture, Kobe University, Rokko, Kobe 657-8501, Japan*
[c] *Molecular Interaction Facility, University of Wisconsin Biotechnology Center, 425 Henry Hall, Madison, WI 53706, USA*

Received 13 December 2005; accepted 5 January 2006

Available online 18 January 2006

Edited by Ulf-Ingo Flügge

Abstract **Calcium-dependent protein kinases (CDPKs) are sensor-transducer proteins capable of decoding calcium signals in diverse phosphorylation-dependent calcium signaling networks in plants and some protists. Using a novel yeast two-hybrid (YTH) approach with constitutively active and/or catalytically inactive forms of AtCPK11 as bait, we identified AtDi19 as an AtCPK11-interacting protein. AtDi19 is a member of a small family of stress-induced genes. The interaction was confirmed using pull-down assays with in vitro translated AtCPK11 and GST–AtDi19 and localization studies in *Arabidopsis* protoplasts cotransfected with AtCPK11:GFP and AtDi19:DsRed2 protein fusions. We further showed that the interaction of AtDi19 is specific to both AtCPK4 and AtCPK11, whereas other closely related CPKs from Arabidopsis interacted weakly (e.g., AtCPK12) or did not interact (e.g., AtCPK26, AtCPK5 and AtCPK1) with AtDi19. Deletion analyses showed that a region containing two predicted nuclear localization signals (NLS) and a nuclear export signal (NES) of AtDi19 is essential for interaction with AtCPK11. We further demonstrated that AtDi19 is phosphorylated by AtCPK11 in a Ca^{2+}-dependent manner at Thr105 and Ser107 within the AtDi19 bipartite NLS using in vitro kinase assays. Our data suggest that disruption of the autoinhibitor domain leading to the formation of a constitutively active CDPK may stabilize kinase–substrate interactions without affecting specificity.**

Keywords: Calcium; Kinase; Signaling; Nucleus; Localization

1. Introduction

Ca^{+2} signaling plays an essential role in a plant's perception and response to biotic and abiotic stimuli as well as in regulating many aspects of growth and development [10,27]. Calcium-dependent protein kinases (CDPKs) are structurally unique Ser/Thr protein kinases that function as sensor-responder molecules to decode calcium dynamics by undergoing calcium-induced conformational changes that activate kinase activity [1,4,11]. CDPKs consist of an N-terminal kinase domain joined to a C-terminal calmodulin-like domain via a junction region that serves to stabilize and maintain the kinase in an autoinhibited state [12,14]. Some CDPK genes are expressed ubiquitously, whereas others are present only in specific tissues or are induced in response to a wide range of hormone, biotic or abiotic stress treatments [13]. Recently, the subcellular localization of 10 members of the Arabidopsis CDPK family has been reported [6,18]. Six members showed plasma membrane localization, two isoforms showed a nuclear and cytosolic distribution, and two other CDPKs localized to the peroxisomes and endoplasmic reticulum, respectively.

Reverse genetic or ectopic expression analysis of a growing number of CDPKs has provided direct evidence for their roles as key regulators in many biological processes [4,10,11,19]. Evidence for a role of CDPKs in biotic stress signaling comes from virus-induced gene silencing experiments of NtCDPK2 in tobacco, which reduced and delayed hypersensitive defense responses to fungal elicitor, whereas ectopic expression of a truncated kinase induced defense responses mediated by ethylene [19,24]. Other studies have provided evidence of the importance of CDPKs in environmental stress signaling pathways. For example, AtCPK10 or AtCPK30 were able to activate the expression of the stress-inducible barley HVA1 promoter [29]. The potential of CDPKs for engineering useful traits has also been suggested by alterations in the expression of rice OsCDPK7 that influenced cold and salt/drought tolerance in transgenic rice plants [25,26]. More recently, AtCPK32 from Arabidopsis was shown to regulate abscisic acid-responsive gene expression via interaction with ABF4, a basic leucine zipper class of transcriptional regulator [5]. RNA interference screens identified a *Medicago truncatula* CDPK (MtCPK1) involved in the control of root hair growth and the regulation of cell wall and defense-related gene expression [7].

One of the most important challenges in the characterization of the physiological functions of CDPKs is the identification of substrates and phosphorylation sites regulated by the different isoforms. It is expected that some CDPKs will be able to phosphorylate many potential substrates, whereas others will have a more limited range of substrate targets [11]. In *Arabidopsis*, only a few substrates have been identified. We have initiated a systematic YTH screening program to identify kinase substrates

*Corresponding author. Fax: +1 775 784 1650.
E-mail address: jcushman@unr.edu (J.C. Cushman).

0014-5793/$32.00
doi:10.1016/j.febslet.2006.01.013

in *Arabidopsis* and to investigate CDPK-mediated signal transduction pathways. In this study, we used constitutively active and/or catalytically impaired versions of AtCPK11 as baits in the YTH system to screen for AtCPK11-interacting proteins and potential substrates. We identified AtDi19, a nuclear protein with two zinc finger-like domains and a member of a small gene family of stress-induced proteins [23], as an AtCPK11-interacting protein. To validate our approach, we demonstrate that constitutively active AtCPK11 interacts with AtDi19 through the same domain that is phosphorylated by the wild type kinase. Our data suggest that a mutation that disrupts the autoinhibitor domain and leads to a constitutively active CDPK may stabilize kinase–substrate interactions without affecting specificity.

2. Materials and methods

2.1. Construction of AtCPK11 mutant baits

Three mutations were generated in the AtCPK11 protein. Substitution of Asp (D) 150 by Ala (A) (AtCPK11-D150A) and of D171 to A (AtCPK11-D171A) resulted in catalytic impairment of the kinase [8]. The change of Phe (F) 306 to A (AtCPK11-F306A) disrupted the autoinhibitor resulting in a constitutively active (partially Ca^{2+}-dependent) kinase [31]. Three different combinations of AtCPK11 mutants were used as baits: AtCPK11-D150A/F306A, AtCPK11-D171A/F306A, and AtCPK11-F306A. Mutations were created using the Quickchange™ site-directed mutagenesis kit according to manufacturer's instructions (Stratagene, La Jolla, CA). The primers used (only the forward primer is shown) were: AtCPK11-D150A, 5′-GGTGTTATGCATAGAGCTCTCAAACCTGAG-3′; AtCPK11-D171A, 5′-GCTTAAGGCTACCGCTTTTGGTTTGTCTG-3′; AtCPK11-F306A, 5′-TCTCGTCTAAAGCAGGCTTCTCAAATGAAT-3′. PCR amplification products of these genes were subcloned into the pBUTE Y2H bait vector to make a GAL4BD fusion protein by recombinational cloning using the following primers: AtCPK11 forward, 5′-CAAAGACAGTTGACTGTATCGCCGGAATTCgagacgaagccaaaccctagacgtccttca-3′; AtCPK11 reverse, 5′–TCAGTATCTACGATTCATAGATCTCTGCAGtcagtcatcagatttttcaccatcaactcc-3′. Uppercase nucleotides are vector target sequence; lowercase amplify bait inserts. Bait plasmids were sequenced to confirm that the inserts were in-frame with the GAL4 DNA-binding domain and transformed into PJ69-4A.

2.2. Yeast two-hybrid analyses

High throughput yeast two-hybrid (Y2H) screens were performed in the University of Wisconsin Molecular Interaction Facility (Madison, WI) according to their methods (http://www.biotech.wisc.edu/mif/). The mutants used as baits in the Y2H screening were cloned into the pBUTE plasmid, a modification of the pBDU-C1 vector [15], constructed by swapping the kanamycin-resistance marker gene for an ampicillin-resistance gene and transformed into the PJ69-4A, *MATa* yeast strain. This strain is unable to grow on medium without Leu, Ura, His, and Ade. The pBUTE plasmid contains the *URA3* gene that allows yeast cells to grow in medium without Ura. Two Arabidopsis cDNA libraries were screened with each bait. One library was prepared from three-day-old etiolated seedlings and the other from three-week-old plants grown on MS agar plates and then subjected to 16 different treatments. Both prey libraries were constructed in pGADT7-Rec using a MATCHMAKER GAL4 Two-Hybrid System 3 kit (Clontech, Mountain View, CA, USA) and introducing the library into yeast strain PJ69-4α. Approximately 18 million clones from each library were screened via mating and selection on Ura/Leu/His drop-out media containing 1 mM 3-amino-1,2,4-triazole (3-AT). Positives were detected by assaying growth (620 nm) and confirmed by assaying for a second yeast reporter via β-galactosidase assays. To validate observed interactions, prey plasmids were isolated, analyzed by restriction digest and representative plasmids were transformed into PJ69-4α. Yeast with preys were mated one-on-one in parallel against the yeast expressing the target baits and the empty bait vector (baits in yeast mating type A).

A second Y2H analysis was performed at the University of Nevada under the same conditions. In order to make valid comparisons among AtCPK11 wild type and mutants, cDNA fragments containing the open reading frame (ORF) of AtCPK11 (wild type and the three mutants) were amplified by PCR and cloned into the pBUTE vector. To generate AtDi19 truncated versions for yeast two-hybrid analysis, cDNA fragments containing different domains of AtDi19 were amplified by PCR and the fragments were inserted into the pGADT7 vector. The constructs were verified by restriction digestion and sequencing.

2.3. Transient expression of GFP and DsRed2 fusion proteins in Arabidopsis protoplasts

The coding region of AtCPK11 (At1g35670) was amplified by PCR and the fragment was inserted into the 35S-sGFP-TYG-NOS (pUC19) plasmid kindly provided by Dr. Jen Sheen (Massachusetts General Hospital, Boston, MA, USA). The resulting construct consisted of AtCPK11 fused to the N-terminus of the GFP protein. AtDi19 was fused to the N-terminus of the DsRed2 protein. The ORF was amplified by PCR and the fragment was inserted into the pDsRed2-1 plasmid (BD Biosciences Inc., Palo Alto, CA, USA). Then, the resulting AtDi19–DsRed2 construct was digested with *Sal*I and *Not*I and the DNA fragment (containing AtDi19 fused to the N-terminus of DsRed2) was inserted into the 35S-sGFP-TYG-NOS plasmid, substituting for the previously described AtCPK11-sGFP fusion protein. Transient expression of GFP and DsRed2 fusion constructs in *Arabidopsis* protoplasts was performed according to Sheen [30]. After 16 h, transformed cells were visualized with a Nikon Eclipse E400 epifluorescence microscope (Nikon Corp., Tokyo, Japan). GFP was visualized with a 450–490 nm excitation filter, a 495 dichroic mirror, and a 500–550 nm emission filter. DsRed2 was visualized with a 528–553 nm excitation filter, a 565 dichroic mirror, and a 600–660 nm emission filter.

2.4. Expression and purification of recombinant proteins

To generate a 6xHis–AtCPK11 fusion protein, the entire ORF of AtCPK11 was amplified by PCR and inserted into the pET30a vector (Novagen Inc., Madison, WI, USA). The respective coding region or sub-domains of AtDi19 was cloned into the pGEX-4T vector (Amersham Biosciences, Piscataway, NJ, USA). Plasmid constructs were transformed into *Escherichia coli* BL21 (DE3) and protein expression was induced by 0.5 mM IPTG for 3 h (2 h for GST or GST fusion peptides) at 30 °C. Purification of recombinant proteins was monitored by 10% SDS–PAGE and in the case of 6xHis–AtCPK11, by Western blot hybridization using a monoclonal anti-6xHis antibody (Covance, Berkeley, CA, USA) used at a 1:1000 dilution and detected with the Western-Light Plus kit (Applied Biosystems, Bedford, MA, USA). 6xHis–AtCPK11 was stored at −20 °C in 50% glycerol, 5 mM HEPES, pH 7.5, and 0.5 μg/μl BSA.

2.5. In vitro binding and phosphorylation assays

The 6xHis–AtCPK11 fusion construct was transcribed and translated in wheat germ extract using the TNT® T7 Coupled Wheat Germ Extract System (Promega, Madison, WI, USA). The pET30a-AtCPK11 plasmid used to purify the His-AtCPK11 protein in *E. coli* was linearized and used as the DNA template. The labeling procedure was performed according to the manufacturer's instructions. Then, the sample was centrifuged at 20 000 × g for 5 min at 4 °C. The binding assay was performed by attaching equimolar amounts of GST–AtDi19 and GST (approximately 20 and 10 μg, respectively) to glutathione sepharose 4B beads and then, a 35 μl aliquot of resin was mixed with 45 μl of TNT® T7 reaction. Samples were rotated for 1 h at 4 °C, pelleted and washed three times with 350 μl of buffer (50 mM HEPES, pH 7.5, 100 mM KCl, 2.5 mM $MgCl_2$, 250 μM EGTA, 350 μM $CaCl_2$, and 2 mM DTT). Proteins were eluted from the resin by adding 35 μl of warm 2× SDS–PAGE sample buffer. Samples were heated at 95 °C for 5 min and proteins were separated by 10% SDS–PAGE. The gel was washed with water for 5 min and incubated in a solution containing 1.65% sodium pyrophosphate and 5% trichloroacetic acid for 15 min. Then, the gel was washed with water for 10 min, dried at 80 °C under vacuum and the ^{35}S labeled proteins were visualized by autoradiography.

In vitro kinase assays were performed in a 20 μl reaction containing 20 mM Tris–HCl, pH 7.5, 10 mM $MgCl_2$, 1 mM EGTA, and 1.1 mM $CaCl_2$. In control reactions, $CaCl_2$ was omitted. Phosphorylation reactions were initiated by adding a mixture of 50 μM ATP and 5 μCi of [γ^{32}P]-ATP and incubated for 20 min at 25 °C. Reactions were stopped

by adding 20 μl of 2× SDS–PAGE sample buffer, heated at 80 °C for 5 min and proteins were separated by 10% SDS–PAGE. Then, the gel was treated as above and the phosphorylated proteins were visualized by autoradiography.

2.6. Mass spectrometry analysis, phosphorylation peptide and site identification

Mass spectrometry (MS) analysis was performed and modified as previously described [3]. After the kinase reaction (6 h), reaction products were dried and the pellet was re-suspended in a trypsin solution containing 100 ng total (0.66 ng/ul) trypsin, (Promega), 14.8 mM ammonium bicarbonate, 2.7 mM dithiothreitol, 7.3 mM iodoacetamide, 0.08% formic acid, 13% acetonitrile, pH 8.0, and incubated for 16 h at 37 °C. The digested peptides were desalted three times, and eluted with conditioning solution (70% acetonitrile, 0.2% formic acid, 5 mg/ml α-Cyano-4-hydroxycinnamic acid), and spotted onto a matrix-assisted laser desorption ionization (MALDI) target using a ZipTip (cat. No. ZTC18M960; Millipore Inc., Billerica, MA, USA). MALDI-time-of-flight (MALDI-TOF) mass spectrometer (MS) analysis of trypsin-digested peptides was performed on a 4700 Proteomics Analyzer (Applied Biosystems, Foster City, CA, USA) at the Proteomics/MS Facility at the University of Nevada, Reno. For Ion-Trap MS/MS analysis, tryptic digested peptides separated by liquid chromatography (Michrom BioResources Inc., Auburn, CA, USA) and analyzed on a coupled nanospray LCQ DECA XP (Thermo Finnigan, San Jose, CA, USA). A neutral loss method [28] was applied to select neutral loss ions. Database searching was performed to identify the phosphorylated peptides. For MALDI-TOF MS data, *m/z* values were searched against the NCBI Ababidopsis database by use of the MS-FIT fingerprinting algorithm (http://prospector.ucsf.edu/ucsfhtml4.0/msfit.htm). For Ion-Trap MS/MS data, *m/z* values of the precursor, y and b ions were searched against the NCBI database by use of the TURBOSEQUEST algorithm (Thermo Finnigan) or MASCOT algorithm (Matrix Science, Boston, MA). In addition, peptides with neutral loss were queried and identified by manual inspection. The MS/MS or MS/MS/MS spectrum of the phosphorylated peptide was inspected manually either compared to the theoretical mass or de novo sequencing by use of DeNovoX (Thermo Finnigan) to confirm the phosphorylation.

3. Results and discussion

3.1. Identification of AtDi19 as an AtCPK11-interacting protein

The *AtCPK11* gene encodes a predicted protein of 495 amino acid containing the well-conserved protein kinase domain (amino acids 26–284) and a C-terminal domain (amino acids 323–495) with four EF-hands involved in calcium binding joined together by an auto-inhibitor or pseudosubstrate domain (amino acids 285–322) (Fig. 1A). The first 25 amino acids

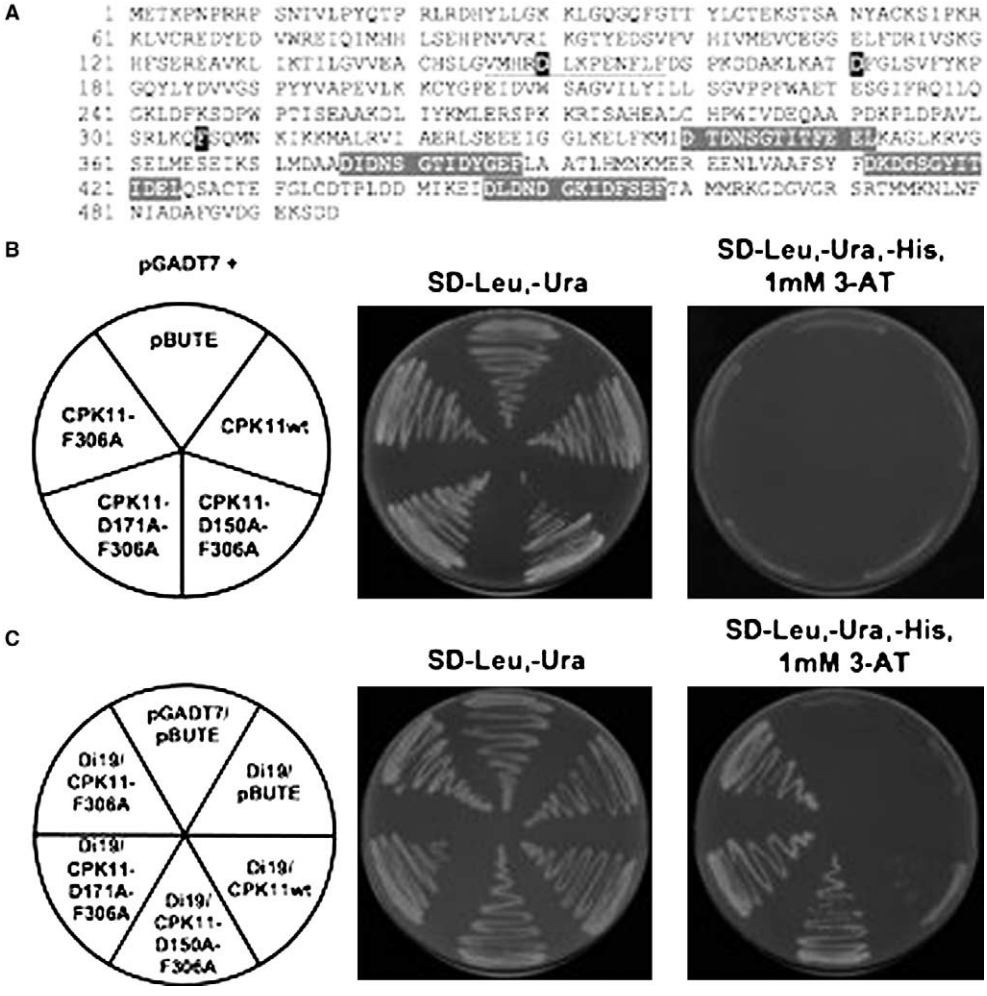

Fig. 1. Design of AtCPK11 bait constructs for YTH screening. (A) Amino acid sequence of the AtCPK11 protein. The three amino acids changed (D150, D171 and F306) for the construction of the YTH baits are indicated by dark shading. The amino acids involved in the active (catalytic) site are underlined and the four EF-hands are indicated by light shading. (B) Auto-induction test of AtCPK11 wild type and mutant baits. The yeast strain PJ69-4A containing the empty vector pGADT7 and either the empty plasmid pBUTE or the pBUTE-AtCPK11 constructs was grown at 30 °C for 4 days in the indicated selective medium. (C) Yeast two-hybrid interactions of wild type and catalytically impaired AtCPK11 mutants with AtDi19. Test constructs were transformed into the yeast strain PJ69-4A and cells were grown at 30 °C for 4 days in the indicated selective medium.

form the N-terminal domain, which is highly variable in both length and sequence in most CDPKs, typically contains subcellular targeting information [13]. However, AtCPK11 is one of only five Arabidopsis CDPKs without a predicted N-terminal myristoylation site (no Gly at position 2) [4].

The yeast-two hybrid system has been previously used to identify substrates for CDPKs [17,21]. In both cases, the efficiency of recovering kinase substrates was improved through the use of truncated versions of the CDPK. For AtCPK11, we tested the hypothesis that the use of catalytically impaired and/or constitutively active variants of AtCPK11 baits would improve the efficiency of recovery of putative prey proteins (see Section 2). None of the three baits were able to auto-induce the His3 reporter gene (Fig. 1B). We identified five clones corresponding to the AtDi19 gene (Dehydration-induced 19, At1g56280) [9]. Moreover, AtDi19 was detected in the screens performed using the three different forms of AtCPK11 baits. Specific interaction between baits and AtDi19 in yeast was confirmed, as yeast co-transformed with the three baits and rescued pGADT7–AtDi19 plasmid were able to grow in selective medium, whereas cells co-transformed with empty vector (pBUTE) and pGADT7–AtDi19 plasmid did not show any indication of interaction (Fig. 1C). AtDi19 interacted strongly with all three mutated versions of AtCPK11, but only very weakly with the wild type kinase (Fig. 1C).

3.2. Recombinant AtCPK11 interacts with AtDi19 in vitro

To validate the interaction of AtCPK11 with AtDi19 observed in the yeast two-hybrid system, we tested the ability of these two proteins to interact using an in vitro "pull-down" assay. 6xHis–AtCPK11 was expressed in the presence of [^{35}S]-Met in a coupled in vitro transcription/translation wheat germ extract system. A full-length protein (~62 kDa) was obtained along with additional lower molecular weight products, which are likely truncation products (Fig. 2). For the interaction assay, [^{35}S]-Met-labeled AtCPK11 was incubated with resin-bound GST–AtDi19 or GST. After washing, the presence of AtCPK11 was clearly detected in the GST–AtDi19 sample showing interaction, whereas binding of AtCPK11 to GST was almost undetectable (Fig. 2).

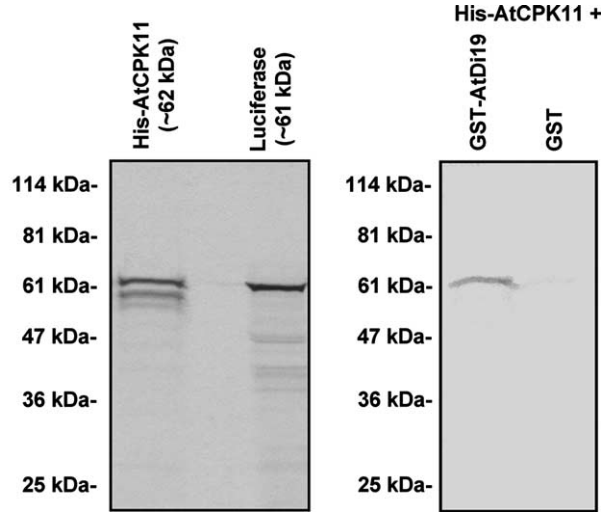

Fig. 2. AtCPK11 and AtDi19 interact in an in vitro protein binding assay. AtCPK11 was labeled with [^{35}S]-Met (left panel shows 5% of the input used in the interaction assay in addition to a luciferase control) and [^{35}S]-Met-labeled AtCPK11 was incubated with immobilized GST–AtDi19 or GST in wheat germ extract. The presence of [^{35}S]-Met-AtCPK11 was detected by autoradiography (right panel). Equimolar amounts of each protein was added to the resin prior to the interaction test.

3.3. Subcellular localization of AtCPK11 and AtDi19

AtCPK11 is one of only a few *Arabidopsis* CDPKs that are not predicted to undergo N-terminal acylation [4]. Like AtCPK4, which is 95% identical to AtCPK11 and has been shown to have a nuclear and cytosolic localization in transgenic *Arabidopsis* plants [6], AtCPK11 lacks an N-terminal acylation consensus motif and contains two potential NLSs, $P_{57}KRK_{60}$ and $P_{268}KKR_{271}$. Thus, AtCPK11 is expected to have a similar subcellular distribution. In agreement with this prediction, we found that AtCPK11–GFP localized throughout the cytoplasm and nucleus in *Arabidopsis* protoplasts (Fig. 3A). The observation that AtCPK11 is localized in both the cytosol and the nucleus suggests that these proteins may shuttle between the cytosol and nucleus. We next studied the subcellular localization of AtDi19 by fusing its complete predicted open reading frame to the N-terminus of DsRed2 protein. The AtDi19–DsRed2 fusion protein displayed a 'speckled' pattern of nuclear localization (Fig. 3B). This localization pattern is consistent with the NLS and NES sequences present in AtDi19 and it would appear that its default localization is nuclear. The presence of both NLS and NES sequences in a protein suggests that its nuclear concentration could be tightly regulated in response to different types of signals through the modulation of both nuclear import and export [22]. Finally, the common localization pattern of both protein

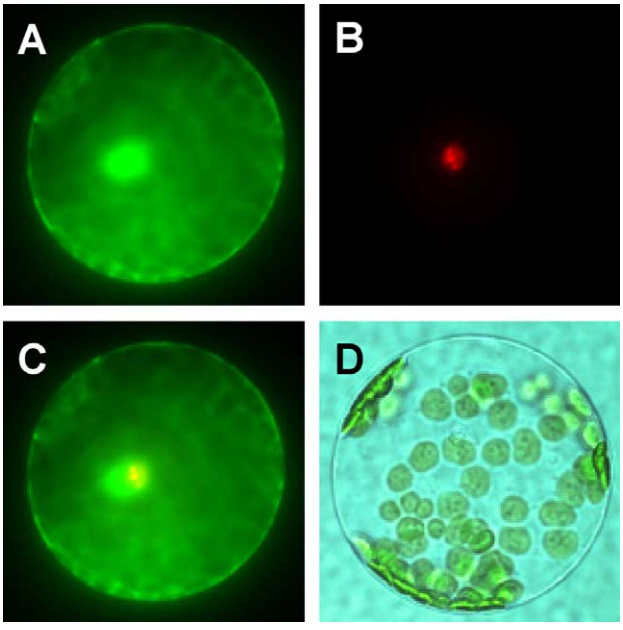

Fig. 3. Subcellular localization of AtCPK11 and AtDi19 using transient expression of *Arabidopsis* mesophyll protoplasts. Protoplasts were transformed with both 35S-AtCPK11:GFP and 35S-AtDi19:DsRed2 and localization of fluorescent signals is shown. (A) Green-channel fluorescent image of protoplast expressing AtCPK11:GFP. (B) Red-channel fluorescent image of the same protoplast shown in A expressing AtDi19:DsRed2. (C) Merged images from A and B. (D) Bright-field image.

fusions (Fig. 3C) is also consistent with interactions occurring between AtCPK11 and AtDi19 in the nucleus, where both AtCPK11 and AtDi19 are present.

3.4. Specificity of the interaction between AtCPK11 and AtDi19

AtCPK11 belongs to a family of 34 CDPKs in Arabidopsis [4,11]. We tested whether other closely related CDPKs could interact with AtDi19 in a YTH system. Constitutively, active forms of five other CDPKs located on the same branch of the CDPK phylogenetic tree group as AtCPK11 (e.g., AtCPK4, AtCPK12, AtCPK26, AtCPK5, and AtCPK1, listed in order of similarity to AtCPK11) [4] were cloned into the pBUTE vector to make GAL4BD fusions and tested for their interaction with AtDi19-GAL4AD (Fig. 4). Interestingly, only AtCPK4 and AtCPK12, which are most similar to AtCPK11, interacted with AtDi19. However, when interaction was tested at a higher stringency (5 mM 3-AT), only AtCPK11 and AtCPK4 interacted with AtDi19, indicating that interaction with these proteins is more specific. None of the kinases showed autoinduction of the His3 gene as bait and, as expected, none of the wild type kinases interacted with AtDi19 (data not shown) under the conditions tested.

The interaction of AtCPK4-F305A with AtDi19 is not surprising, as AtCPK11 and AtCPK4 are two of the most closely related CDPKs in Arabidopsis. However, both proteins may undergo different regulation in the plant. The weak interaction detected between AtCPK12-F302A and AtDi19 is consistent with the above observations as this kinase is the next most closely related member of the CDPK superfamily. Our study also included the constitutively active forms of AtCPK1, demonstrated previously to be partially Ca^{+2} independent [31], and AtCPK26, another soluble CDPK highly similar to AtCPK11 with the same subcellular localization pattern as AtCPK4 and AtCPK11 (Dr. Naomi Etheridge, unpublished data). Taken together, our results indicate that constitutively active CDPKs can be used to identify interaction partners that are specific for a particular CDPK (or its closely-related homologs).

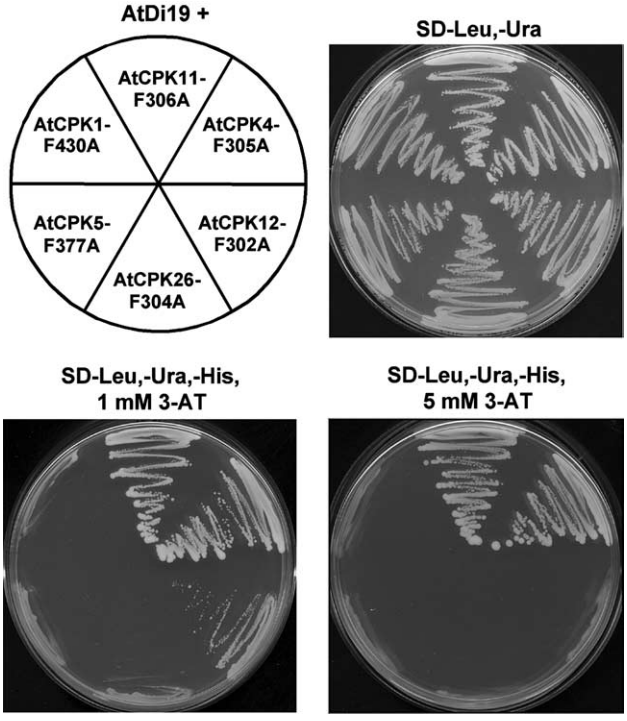

Fig. 4. Specificity of the interaction between AtCPK11 and AtDi19. Constitutively active forms of five CDPKs in the same phylogentic group as AtCPK11 (e.g., AtCPK4 (*At4g09570*), AtCPK12 (*At5g23580*), AtCPK26 (*At4g38230*), AtCPK5 (*At4g35310*), and AtCPK1 (*At5g04870*), listed in order of similarity to AtCPK11) were cloned into the pBUTE vector to make GAL4BD fusions and their interaction with AtDi19-GAL4AD was compared to the constitutively active form of AtCPK11. Test constructs were transformed into the yeast strain PJ69-4A and cells were grown at 30 °C for 6 days in the indicated selective medium.

3.5. Mapping binding sites on AtDi19

During yeast two-hybrid screening, we observed that one of the five AtDi19 prey clones encoded only the first 128 amino acids of the AtDi19 protein and lacked the C-terminal domain of 78 amino acids. This observation suggested that the interaction with AtCPK11 could occur through the N-terminal segment of the protein. To identify the AtDi19 region responsible for the interaction with AtCPK11, the full-length *AtDi19* (206 aa) and five deletion constructs were cloned into pGADT7, and introduced into yeast cells together with the pBUTE-AtCPK11-F306A plasmid (Fig. 5A). AtDi19 deletion constructs in the presence of empty bait vector were not able to grow on His medium (Fig. 5B). Removal of the C-terminal domain of AtDi19 (AtDi19-1–128), which did not prevent interaction with AtCPK11, suggests that this C-terminal domain (AtDi19-129–206) is not necessary for interaction (Fig. 5B). This was further confirmed by the lack of interaction between AtCPK11 and the AtDi19-129–206 construct. In addition, N-terminal 32 residues of AtDi19 do not appear to participate in the interaction with AtCPK11 either, because the interaction of AtCPK11 with a construct lacking this and the C-terminal regions (AtDi19-33–128) was as strong as with the full-length AtDi19. The central region of AtDi19 (AtDi19-33–128) contains a domain with two C2H2-like zinc fingers (amino acids 33–92). In addition, it contains a monopartite NLS ($R_{93}KRK_{96}$) and a bipartite NLS (R_{98}KSGTNSTLSLLRKELR$_{114}$) predicted by the PSORT software [20] (http://psort.nibb.ac.jp). Moreover, a leucine-rich sequence ($\underline{L}_{113}$REGD$\underline{L}$QR$\underline{L}_{121}$) was predicted to be a putative NES by the NetNES software [16] (http://www.cbs.dtu.dk/services/NetNES/). We tested the interaction of the Zn finger domains and the NLS/NES sequences with AtCPK11 and determined that the NLS/NES region was necessary and sufficient for interaction with the kinase, although this interaction was slightly weaker than if both Zn finger domains and the NLS/NES region were present (Fig. 5B). Taken together, these deletion analyses indicate that AtCPK11 may interact with AtDi19 through the NLS–NES region, although we cannot preclude a role for the zinc finger-like domains in the interaction with AtCPK11.

3.6. Recombinant AtCPK11 phosphorylates AtDi19 in vitro

To determine if AtDi19 is a substrate of AtCPK11, we tested its ability to be phosphorylated by AtCPK11 using an in vitro kinase assay. Recombinant His-tagged-AtCPK11 and GST–AtDi19 were expressed in *E. coli* and purified by affinity chromatography (Fig. 6A). Recombinant AtCPK11 phosphorylated GST–AtDi19 after a short incubation period with [γ^{32}P]-ATP (Fig. 6B), corroborating the interaction observed in previous assays. Autophosphorylation of 6xHis–AtCPK11

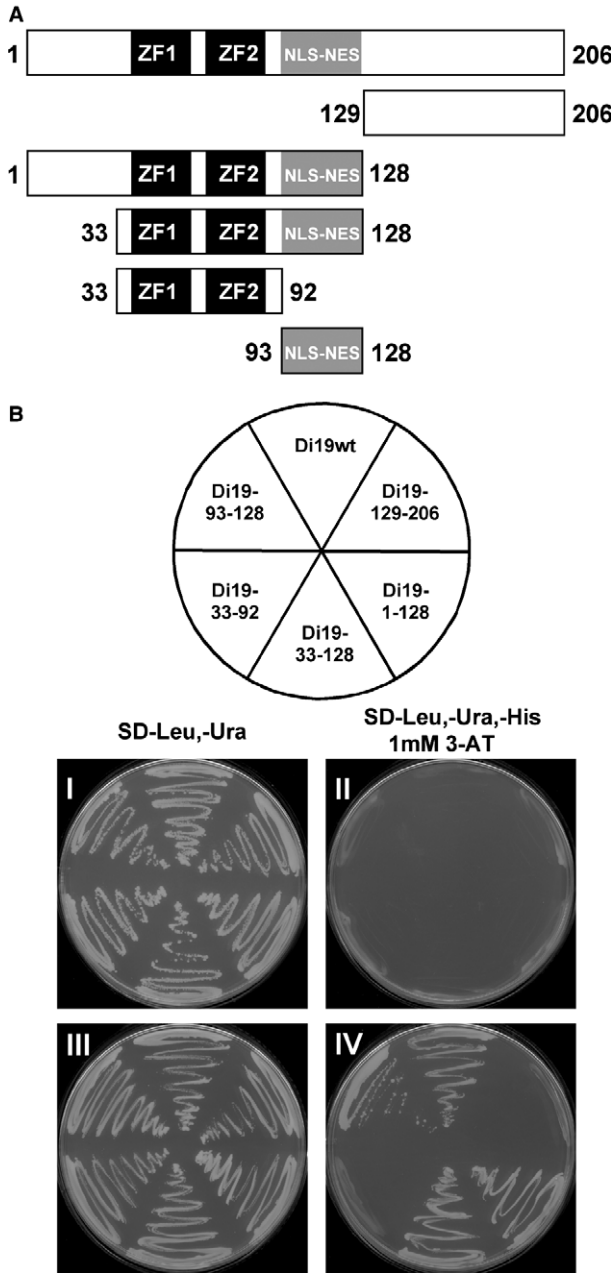

Fig. 5. Schematic diagram of plasmid constructs for mapping AtDi19 domains involved in the interaction with AtCPK11. (A) A series of constructs carrying various AtDi19 N-terminal and/or C-terminal deletions were generated as GAL4AD fusions. Zinc finger domains ZF1 and ZF2 are indicated by dark boxes and the NLS–NES region is indicated by light box. (B) Full-length AtDi19 and deletion constructs were tested in combination with the GAL4BD alone (panels I and II) or the GAL4BD:AtCPK11-F306A fusion (panels III and IV). After constructs were transformed into the yeast strain PJ69-4A, the cells were grown at 30 °C for 9 days in the indicated selective medium.

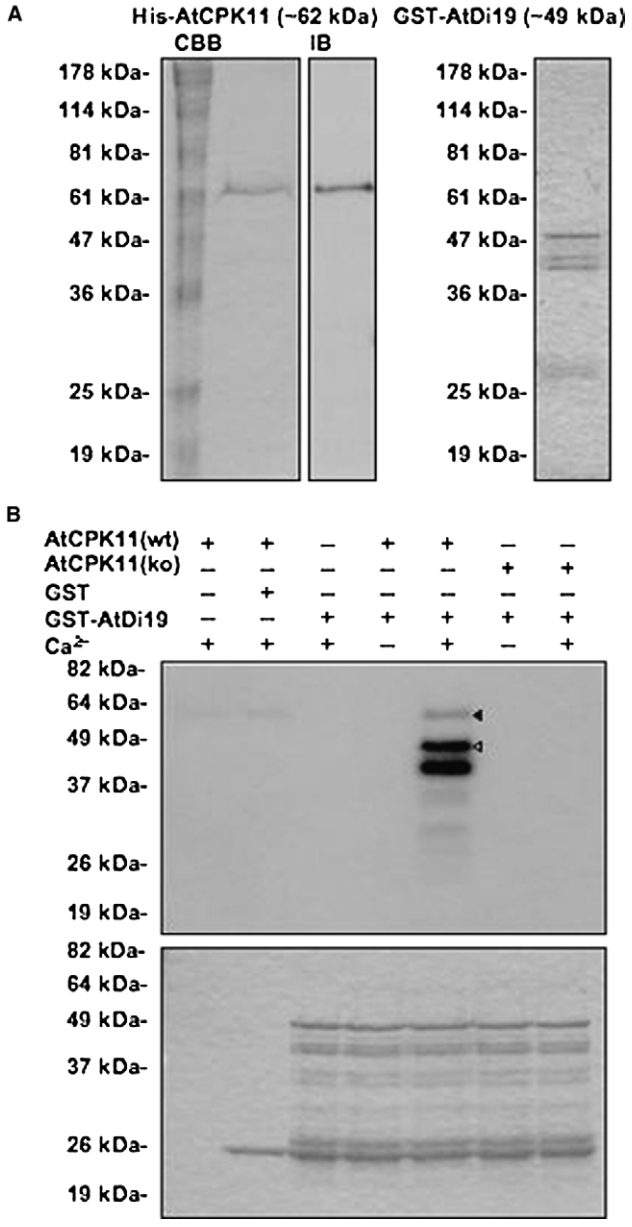

Fig. 6. AtDi19 is phosphorylated by AtCPK11 in vitro. (A) Purification of AtCPK11 and AtDi19 recombinant proteins. The purified His-AtCPK11 recombinant protein is shown in a Coomassie Brilliant Blue-stained gel (CBB) and in a Western blot detected with anti-His tag antibody (IB) (left panel). A CBB-stained gel containing GST–AtDi19 protein is also shown (right panel). (B) AtCPK11 phosphorylates AtDi19 in vitro. Autophosphorylation of His-AtCPK11 is indicated by a closed arrowhead, whereas phosphorylation of full-length GST–AtDi19 is indicated by an open arrow head (upper panel). AtCPK11 (ko) indicates a catalytically inactive form of His-AtCPK11 containing the D150A mutation. CBB-stained gel of panel A showing GST and GST–AtDi19 staining (lower panel). AtCPK11 isoforms are not evident as only 10 ng were used to obtain a kinase:substrate ratio of 1:100. Note that molecular weight markers are slightly different between panels A and B because different batches of ladder were used

was more evident when it was incubated with the GST–AtDi19 fusion protein than when 6xHis–AtCPK11 was incubated alone or with GST (Fig. 6B). This suggests that autophosphorylation of AtCPK11 is enhanced upon binding to the substrate. Autophosphorylation and substrate phosphorylation were Ca^{+2}-dependent (Fig. 6B). As expected, no phosphorylation of GST–AtDi19 was observed when it was incubated with AtCPK11 containing the D150A mutation, which conferred a catalytically inactive kinase. This result demonstrated that GST–AtDi19 is phosphorylated by AtCPK11. Taken together, these results indicate that AtDi19 can interact with and be phosphorylated by AtCPK11 in a Ca^{+2}-dependent manner.

3.7. AtDi19 bipartite NLS is phosphorylated by AtCPK11 in vitro

Recently, mass spectrometry has been widely used to identify proteins and post-translational modification of proteins [2]. To identify potential AtDi19 residues phosphorylated by AtCPK11 we performed MALDI-TOF MS and Ion-Trap LC/MS/MS. MALDI-TOF MS analysis identified a phosphorylated peptide within AtDi19 bipartite NLS sequence. The *m/z* and amino acid sequence of the peptide was 1599.7 and S_{97}RKSGTNSTLSLLR$_{110}$, respectively (data not shown). The phosphorylated residues of the peptide could not be unambiguously determined. In addition, LC/MS/MS analysis identified another phosphorylated peptide. The *m/z* and amino acid sequence of the peptide was 1356.6 and S_{100}GTNSTLSLLRK$_{111}$, respectively. The MS/MS data showed that Ser_{100} and Thr_{102} were not phosphorylated. Nevertheless, the phosphorylation of Ser_{104}, Thr_{105} and Ser_{107} could not be unambiguously determined, which indicated that AtCPK11 may phosphorylate within the AtDi19 bipartite NLS at multiple residues. This hypothesis was further confirmed by in vitro kinase assays using the peptide S_{100}GTNSTLSLLR$_{110}$ fused to GST as a substrate. We demonstrated that this wild type peptide was phosphorylated by AtCPK11 in vitro (K_m = 25 μM) (Fig. 7A). This K_m value is within the expected range for a protein to be considered a good substrate for a CDPK [10]. As expected, no phosphorylation of GST–AtDi19 was observed when it was incubated with AtCPK11 containing the D150A mutation (data not shown). In addition, using the same peptide containing individual mutations of Ser_{104}, Thr_{105} and Ser_{107} to Ala we showed that one or both Thr_{105} and Ser_{107} are the preferred sites phosphorylated by AtCPK11 as mutations of these residues reduced phosphorylation of the peptide to only 30% and 23% relative to the wild type, respectively (Figs. 7A and B). The S_{107}LLR$_{110}$ motif resembles a typical phosphorylation site for CDPKs (S-X-X-Basic) [10], but the Thr_{105} site appears to be novel.

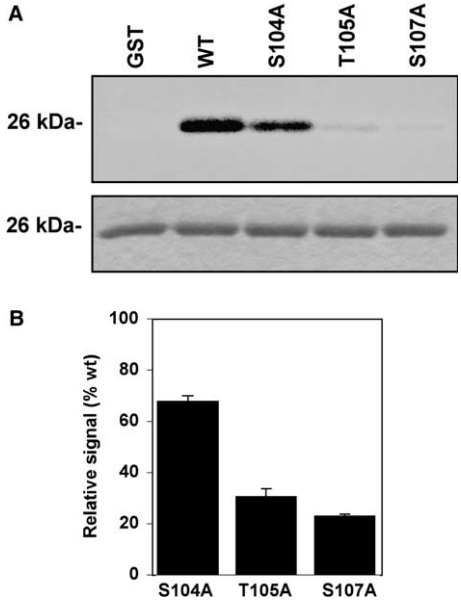

Fig. 7. AtDi19 bipartite NLS is phosphorylated by AtCPK11. (A) in vitro phosphorylation of the S_{100}GTNSTLSLLR$_{110}$ peptide and effect of mutation of specific amino acids on the phosphorylation of the peptide by AtCPK11. The autoradiogram (top panel) shows the phosphorylation of several GST fusion peptides containing the sequence S_{100}GTNSTLSLLR$_{110}$ (WT) or the indicated mutations. A GST control was also included (GST). The CBB-stained gel of the top panel is also shown (bottom panel). Note that the control GST protein contains the amino acid sequence encoded by the multi-cloning site. (B) Quantification of the signals obtained in (A) was done using a phosphorimager. The figure presents the means ± S.E. (n = 3).

3.8. Conclusions

There are two major conclusions that can be drawn from this study. First, our data suggest that the AtCPK11-F306A mutation makes the interaction of the kinase with AtDi19 (and possibly with other substrates) more stable (Fig. 1). Second, to validate our approach, we have demonstrated that constitutively active AtCPK11 interacts with AtDi19 through the same domain that is phosphorylated by the wild type kinase. These results, together with the analysis of the interaction of similar CDPKs with AtDi19 suggest that disruption of the autoinhibitor does not affect the specificity of the kinase for its substrate. Thus, it is possible that the same approach could be used to improve the efficiency of identifying candidate substrates for other CDPKs.

Acknowledgments: This work was supported in part by the National Science Foundation Grant No. MCB-0114769, and the Nevada Agricultural Experiment Station, and is published as publication No. 03066814 of the University of Nevada Agricultural Experiment Station. We thank Dr. Jen Sheen (Massachusetts General Hospital, Boston, MA) for providing the 35S-sGFP-TYG-NOS plasmid. We thank Mary Ann Cushman, Jennifer Welser, Yongil Yang, Alicia M. Rodriguez Huete (University of Nevada, Reno), Dr. Wassim Chehab (University of California, Davis), and Dr. Rahul Patharkar (Massachusetts General Hospital, Boston, MA) for technical assistance and valuable suggestions. The authors thank Drs. J.F. Harper (University of Nevada) and J.C. Thomas (University of Michigan) for critical reading of the manuscript.

References

[1] Asano, T., Tanaka, N., Yang, G., Hayashi, N. and Komatsu, S. (2005) Genome-wide identification of the rice calcium-dependent protein kinase and its closely related kinase gene families: comprehensive analysis of the CDPKs gene family in rice. Plant Cell. Physiol. 46, 356–366.

[2] Aebersold, R. and Mann, M. (2003) Mass spectrometry-based proteomics. Nature 422, 198–207.

[3] Chang, I.F., Szick-Miranda, K., Pan, S. and Bailey-Serres, J. (2005) Proteomic characterization of evolutionarily conserved and variable proteins of Arabidopsis cytosolic ribosomes. Plant Physiol. 137, 848–862.

[4] Cheng, S.H., Willmann, M.R., Chen, H.C. and Sheen, J. (2002) Calcium signaling through protein kinases: the Arabidopsis calcium-dependent protein kinase gene family. Plant Physiol. 129, 469–485.

[5] Choi, H.I., Park, H.J., Park, J.H., Kim, S., Im, M.Y., Seo, H.H., Kim, Y.W., Hwang, I. and Kim, S.Y. (2005) Arabidopsis calcium-dependent protein kinase AtCPK32 interacts with ABF4, a transcriptional regulator of abscisic acid-responsive gene expression, and modulates its activity. Plant Physiol. 139, 1750–1761.

[6] Dammann, C., Ichida, A., Hong, B., Romanowsky, S., Hrabak, E., Harmon, A., Pickard, B. and Harper, J. (2003) Subcellular targeting of nine calcium-dependent protein kinase isoforms from Arabidopsis. Plant Physiol. 132, 1840–1848.

[7] Ivashuta, S., Liu, J., Liu, J., Lohar, D.P., Haridas, S., Bucciarelli, B., Vandenbosch, K.A., Vance, C.P., Harrison, M.J. and Gantt, J.S. (2005) RNA interference identifies a calcium-dependent protein kinase involved in *Medicago truncatula* root development. Plant Cell 17, 2911–2921.

[8] Gibbs, C.S. and Zoller, M.J. (1990) Rational scanning of a protein kinase identifies functional regions involved in catalysis and substrate interactions. J. Biol. Chem. 266, 8923–8931.

[9] Gosti, F., Bertauche, N., Vartanian, N. and Giraudat, J. (1995) Abscisic acid-dependent and -independent regulation of gene expression by progressive drought in *Arabidopsis thaliana*. Mol. Gen. Genet. 246, 10–18.
[10] Harper, J.F. and Harmon, A. (2005) Plants, symbiosis and parasites: a calcium signalling connection. Nat. Rev. Mol. Cell. Biol. 6, 555–566.
[11] Harper, J.F., Breton, G. and Harmon, A. (2004) Decoding Ca^{2+} signals through plant protein kinases. Annu. Rev. Plant. Biol. 55, 263–288.
[12] Harper, J.F., Huang, J.F. and Lloyd, S.J. (1994) Genetic identification of an autoinhibitor in CDPK, a protein kinase with a calmodulin-like domain. Biochemistry 33, 7267–7277.
[13] Hrabak, E.M., Chan, C.W.M., Gribskov, M., Harper, J.F., Choi, J.H., Halford, N., Kudla, J., Luan, S., Nimmo, H.G., Sussman, M.R., Thomas, M., Walker-Simmons, K., Zhu, J.-K. and Harmon, A.C. (2003) The Arabidopsis CDPK-SnRK superfamily of protein kinases. Plant Physiol. 132, 666–680.
[14] Huang, J.F., Teyton, L. and Harper, J.F. (1996) Activation of a Ca(2+)-dependent protein kinase involves intramolecular binding of a calmodulin-like regulatory domain. Biochemistry 35, 13222–13230.
[15] James, P., Halladay, J. and Craig, E.A. (1996) Genomic libraries and a host strain designed for highly efficient two-hybrid selection in yeast. Genetics 144, 1425–1436.
[16] la Cour, T., Kiemer, L., Mølgaard, A., Gupta, R., Skriver, K. and Brunak, S. (2004) Analysis and prediction of leucine-rich nuclear export signals. Protein Eng. Des. Sel. 17, 527–536.
[17] Lee, S.S., Cho, H.C., Yoon, G.M., Ahn, J.-W., Kim, H.-H. and Pai, H.S. (2003) Interaction of NtCDPK1 calcium-dependent protein kinase with NtRpn3 regulatory subunit of the 26S proteasome in *Nicotiana tabacum*. Plant J. 33, 825–840.
[18] Lu, S.X. and Hrabak, E.M. (2002) An Arabidopsis calcium-dependent protein kinase is associated with the endoplasmic reticulum. Plant Physiol. 128, 1008–1021.
[19] Ludwig, A.A., Saitoh, H., Felix, G., Freymark, G., Miersch, O., Wasternack, C., Boller, T., Jones, J.D. and Romeis, T. (2005) Ethylene-mediated cross-talk between calcium-dependent protein kinase and MAPK signaling controls stress responses in plants. Proc. Natl. Acad. Sci. USA 102, 10736–10741.
[20] Nakai, K. and Kanehisa, M. (1992) A knowledge base for predicting protein localization sites in eukaryotic cells. Genomics 14, 897–911.
[21] Patharkar, O.R. and Cushman, J.C. (2000) A stress-induced calcium-dependent protein kinase from *Mesembryanthemum crystallinum* phosphorylates a two-component pseudo-response regulator. Plant J. 24, 679–691.
[22] Poon, I.K.H. and Jans, D.A. (2005) Regulation of nuclear transport: central role in development and transformation? Traffic 6, 173–186.
[23] Rodriguez Milla, M.A., Townsend, J., Chang, I.-F. and Cushman, J.C. (in press) The Arabidopsis AtDi19 gene family encodes a novel type of Cys2/His2 zinc-finger protein implicated in ABA-independent dehydration, high-salinity stress and light signaling pathways. Plant Mol. Biol., in press.
[24] Romeis, T., Ludwig, A.A., Martin, R. and Jones, J.D. (2001) Calcium-dependent protein kinases play an essential role in a plant defence response. EMBO J. 20, 5556–5567.
[25] Saijo, Y., Hata, S., Kyozuka, J., Shimamoto, K. and Izui, K. (2000) Over-expression of a single Ca^{2+}-dependent protein kinase confers both cold and salt/drought tolerance on rice plants. Plant J. 3, 19–27.
[26] Saijo, Y., Kinoshita, N., Ishiyama, K., Hata, S., Kyozuka, J., Hayakawa, T., Nakamura, T., Shimamoto, K., Yamaya, T. and Izui, K. (2001) A Ca^{2+}-dependent protein kinase that endows rice plants with cold- and salt-stress tolerance functions in vascular bundles. Plant Cell. Physiol. 42, 1228–1233.
[27] Sanders, D., Pelloux, J., Brownlee, C. and Harper, J.F. (2002) Calcium at the crossroads of signaling. Plant Cell 14, 401–417.
[28] Schroeder, M.J., Shabanowitz, J., Schwartz, J.C., Hunt, D.F. and Coon, J.J. (2004) A neutral loss activation method for improved phosphopeptide sequence analysis by quadruple ion trap mass spectrometry. Anal. Chem. 76, 3590–3598.
[29] Sheen, J. (1996) Ca^{2+}-dependent protein kinases and stress signal transduction in plants. Science 274, 1900–1902.
[30] Sheen, J. (2002) A transient expression assay using Arabidopsis mesophyll protoplasts. Available from: <http://genetics.mgh.harvard.edu/sheenweb/>.
[31] Vitart, V., Christodoulou, J., Huang, J.F., Chazin, W.J. and Harper, J.F. (2000) Intramolecular activation of a Ca^{2+}-dependent protein kinase is disrupted by insertions in the tether that connects the calmodulin-like domain to the kinase. Biochemistry 39, 4004–4011.